

CHAPTER 26

A METHOD OF NUMERICAL ANALYSIS OF WAVE PROPAGATION --- APPLICATION TO WAVE DIFFRACTION AND REFRACTION ---

by

Yoshiyuki ITO* and Katsutoshi TANIMOTO*

ABSTRACT

A method is presented to obtain numerically wave patterns in the region of arbitrary shape. The principle is to solve the linearized wave equations under given boundary conditions from a certain initial state.

In this paper, two principal applications of our method of numerical analysis are presented in the fundamental fashion.

The first application of our method is related to wave diffraction. The distribution of wave height along a semi-infinite breakwater and a detached breakwater is calculated and compared with that obtained from the conventional analytic solutions to confirm the validity of our numerical method. Three examples of application are presented to the wave height distribution along breakwaters of arbitrary shape and of arbitrary reflecting power and to wave force upon a large isolated vertical structure.

The second application is to wave refraction. In particular, this method of numerical analysis is applicable to the analysis of wave propagation in the region of ray intersections which are indicated by the conventional geo-optic wave refraction theory. An example of application to a submerged shoal with concentric circular contours where a cusped caustic is formed is presented and the calculated wave height distribution around the shoal is compared with that obtained from hydraulic model experiments.

Our method of numerical analysis might be applied to the calculation of wave height distribution in the region of more realistic bottom topography and it is possible to include vertical boundaries of arbitrary shape.

1. INTRODUCTION

When we examine the calmness in a harbour with respect to the sheltering effect of breakwaters, only the consideration of wave diffraction is not sufficient, but the effect of reflected waves from other boundaries and water depth variation in the harbour should be taken into account.

* Hydraulic Engineering Division, Port and Harbour Research Institute, Ministry of Transport, 3-1-1, Nagase, Yokosuka, Japan.

In most cases, a realistic wave height distribution in a harbour is obtained by the performance of hydraulic model tests. If we could treat theoretically together with all factors of disturbance in a harbour as diffraction, reflection, and refraction of waves, it will be of great help for the examination of an appropriate arrangement of breakwaters.

From such a standpoint, recent studies in France are noticeable by Biesel and Ranson(1), Gaillard(2), and Barailler and Gaillard(3). In these papers, examples of calculation of wave height distribution in an arbitrary shape harbour of constant or variable water depth are presented. Most recently, Berkhoff(4) has discussed the computation of combined refraction-diffraction. All of these methods of calculation are to solve basic wave equations as a boundary value problem.

On the other hand, the authors have studied to obtain the height and flow distribution of long waves in an arbitrary shape harbour from the standpoint of the effect of breakwaters against tsunamis, since the Chilian Earthquake Tsunami in 1960(5-8). In this method, a train of tsunamis is supposed to propagate into a calm region and the solution both in transient state and in stationary state can be obtained by calculating step by step the basic hydrodynamic equations for long waves under the given boundary conditions from a certain initial state.

In this paper, this method of numerical analysis have developed so as to be applicable to waves in any region from deep water to shallow water. For short waves, since it is an aim, in general, to obtain the solution in stationary state, the calculation in transient state can be regarded as a process to reach the end, whereas in case of tsunamis the transient state is significant as an actual phenomenon.

The basic equations in our numerical analysis method are the linearized wave equations including unknown functions at the water surface only such as the water surface elevation and the components of particle velocity, which are derived on the basis of a small amplitude assumption in a constant water depth from the Eulerian equations of motion and of continuity.

The wave height distribution around an arbitrary alignment of breakwaters can be obtained by the application of our method of numerical analysis and it is not difficult to include other vertical walls behind the breakwaters. For a simple alignment of breakwater, the effect of reflecting power can be included in the diffraction diagram by our modified calculation method which is named the "Wave generator method". This modified method is based on the principle that the effect of breakwater is equivalent to a hypothetical wave generator which makes the corresponding reflecting waves at the front face and waves cancelling the incident waves at the rear face of the breakwater.

Since it is not irrational to loose the condition of constant water depth to variable water depth, as far as the variation of water depth is gentle. In particular, an interesting application of our method is the analysis of wave propagation in the vicinity of caustics where ray intersections occur. It has been pointed out that the conventional geo-optic wave refraction theory fails to predict the wave height at and near caustics. Pierson(9) has discussed the existence of caustics and suggested some theoretical approaches for the solution of the caustic problem. Our basic wave equations are equivalent to what Pierson has suggested as the general basic equation of wave refraction.

For a smooth caustic, Chao(10) has developed the uniform asymptotic solution, and Chao and Pierson(11) have compared the calculated wave heights with those obtained by hydraulic model tests for a straight caustic. Most recently, Whalin(12) has pointed out that the effect of diffraction in wave refraction is vividly significant in the vicinity of a cusped caustics from his results of model experiments, and Biesel(13) has discussed the general calculation method of wave refraction including the effect of diffraction as a boundary value problem.

In this paper, several examples of application of our numerical analysis method are presented in the fundamental fashion to demonstrate its applicability to various problems of wave propagation. Being associated to wave diffraction, calculations of wave height distribution along a breakwater and of wave force upon a large isolated vertical structure are shown. As to wave refraction, an example of application to the wave height distribution around a submerged shoal with concentric circular contours where the conventional geo-optic refraction theory indicates the formation of a cusped caustics and the calculated wave heights are compared with those obtained by hydraulic model experiments.

2. BASIC EQUATIONS

2.1 Equations of motion and of continuity and boundary conditions

Propagation of small amplitude waves in the region of constant water depth of ideal fluid is treated in this analysis and irrotational motion is assumed.

The Eulerian equations of motion and of continuity and boundary conditions at the water surface and the bottom for a linearized wave are as follows;

$$\left. \begin{aligned} \frac{\partial u}{\partial t} &= - \frac{1}{\rho} \frac{\partial p}{\partial x} \\ \frac{\partial v}{\partial t} &= - \frac{1}{\rho} \frac{\partial p}{\partial y} \\ \frac{\partial w}{\partial t} &= - \frac{1}{\rho} \frac{\partial p}{\partial z} - g \end{aligned} \right\} \quad (2.1)$$

$$\frac{\partial u}{\partial x} + \frac{\partial v}{\partial y} + \frac{\partial w}{\partial z} = 0 \quad (2.2)$$

$$p = 0, \quad \text{at } z = \eta \quad (2.3)$$

$$w = \frac{\partial \eta}{\partial t}, \quad \text{at } z = \eta \quad (2.4)$$

$$w = 0, \quad \text{at } z = -h \quad (2.5)$$

where u,v,w are components of water particle velocity, p is pressure, η is water surface elevation, and h is water depth.

2.2 Derivation of basic wave equations at water surface

Equations (2.1) ~ (2.5) are transformed into the wave equations including only unknown functions at the water surface, which can be solved by a numerical method. For convenience sake of transformation, the motion is considered in the field of a velocity potential.

The velocity potential in a constant water depth can be expressed in the following form, after considering the bottom boundary condition of Eq.(2.5),

$$\phi = \psi(x,y,t) \cosh k(h+z) \quad (2.6)$$

where k is a constant. Equation (2.6) is different a little from the ordinary one, since a term on time t is not separated off.

Using this velocity potential, the components of water particle velocity can be written as follows;

$$\left. \begin{aligned} u &= \frac{\cosh k(h+z)}{\cosh kh} u_0(x,y,t) \\ v &= \frac{\cosh k(h+z)}{\cosh kh} v_0(x,y,t) \\ w &= \frac{\sinh k(h+z)}{\sinh kh} w_0(x,y,t) \end{aligned} \right\} \quad (2.7)$$

where u_0, v_0, w_0 are the components of unknown water particle velocity at the water surface.

Now, consider the pressure p .

By integrating equations of motion into which the velocity potential of Eq.(2.6) is substituted, we get

$$-\cosh k(h+z) \frac{\partial \psi}{\partial t} + \frac{p}{\rho} + gz = 0$$

Considering the free surface condition of Eq.(2.3), following well known relation of the pressure p is obtained,

$$p = \rho g \frac{\cosh k(h+z)}{\cosh kh} \eta(x,y,t) - \rho gz \quad (2.8)$$

Since w_0 in the Eq.(2.7) is given by the kinematic boundary condition at the water surface of Eq.(2.4), the unknown functions u, v, w and p in the original basic equations have been represented by a constant k and the unknown functions u_0, v_0 , and η at the water surface. By substituting these relations into the first and the second equation of Eq.(2.1) and into Eq.(2.2), following modified equations of motion and of continuity are derived,

$$\left. \begin{aligned} \frac{\partial u_0}{\partial t} &= -g \frac{\partial \eta}{\partial x} \\ \frac{\partial v_0}{\partial t} &= -g \frac{\partial \eta}{\partial y} \\ \frac{\partial \eta}{\partial t} &= -\frac{1}{k} \tanh kh \left(\frac{\partial u_0}{\partial x} + \frac{\partial v_0}{\partial y} \right) \end{aligned} \right\} \quad (2.9)$$

These are the basic wave equations at the water surface in our analysis.

From the third equation of Eq.(2.1), the following relation is obtained for a constant value k,

$$\frac{\partial \eta^2}{\partial t^2} = -kg \tanh kh \cdot \eta$$

When η has a period T ($= 2\pi / \sigma$), this relation is equivalent to

$$\sigma^2 = kg \tanh kh \tag{2.10}$$

This is the well-known relationship between the wave period and the wave length in the conventional small amplitude wave theory, if the k is interpreted as the wave number $2\pi/L$.

An arbitrary profile wave can be considered as a composite wave of such components of which each satisfies the relation of Eq.(2.10) respectively.

2.3 Non-dimensional basic wave equations

It is advantageous to perform calculation in a non-dimensional system, because of the generality of results. To obtain the non-dimensional wave equations, we introduce the non-dimensional variables defined by,

$$\left. \begin{aligned} x_* &\equiv \frac{x}{L} = \frac{x}{cT} \\ y_* &\equiv \frac{y}{L} = \frac{y}{cT} \\ t_* &\equiv \frac{t}{T} \end{aligned} \right\} \tag{2.11}$$

$$\left. \begin{aligned} u_* &\equiv \frac{u_0}{ag/c} \\ v_* &\equiv \frac{v_0}{ag/c} \\ \eta_* &\equiv \frac{\eta}{a} \end{aligned} \right\} \tag{2.12}$$

where a is the amplitude of incident waves.

Substituting these relations into Eq.(2.10), the following non-dimensional wave equations are obtained,

$$\left. \begin{aligned} \frac{\partial u_*}{\partial t_*} &= -\frac{\partial \eta_*}{\partial x_*} \\ \frac{\partial v_*}{\partial t_*} &= -\frac{\partial \eta_*}{\partial y_*} \\ \frac{\partial \eta_*}{\partial t_*} &= -\frac{\partial u_*}{\partial x_*} - \frac{\partial v_*}{\partial y_*} \end{aligned} \right\} \tag{2.13}$$

3. METHOD OF NUMERICAL CALCULATION

3.1 Computing region

Let us consider a simple example where incident waves are progressing normally to a semi-infinite breakwater and suppose we intend to obtain only the distribution of wave height along the breakwater.

We may consider the propagation of waves around the breakwater, in the sense of geometrics, to resolve into incident waves, reflected waves, and diffracted waves as shown in Fig.-3.1.

Since we are going to calculate only the wave height along the breakwater, it is sufficient if computing points of water elevation are included in an effective computing region. To continue calculations for the pur incident waves, however, wider region than the effective region must be considered as a computing region. In our calculation, a rectangular computing region is adopted as shown in Fig.-3.2, of which the circumference boundary is a wall reflecting the incoming waves perfectly. This boundary is an imaginary boundary, because it is only for the performance of calculation.

The required region for computing depends on the alignment of breakwater, the direction of incident waves, and the length of breakwater for which effective calculation should be made. In this example, since there exists no obstruction up to the front of breakwater, initial conditions can be given as a state when the front of incident wave trains have reached the breakwater.

Suppose we are going to calculate effectively over two wave length from the tip of the breakwater. Then, it is sufficient if the calculation is continued over four periods from the initial state, and the rectangular imaginary boundary can be put as shown in Fig.-3.2. In this figure, the propagation pattern of diffracted waves from the tip of breakwater (real line) and its reflection pattern from the imaginary boundary (dotted line) are shown. Patterns of incident waves and reflected waves from the breakwater can be drawn in a similar way and these reflected waves by the imaginary boundary reach around the breakwater after four periods calcu-

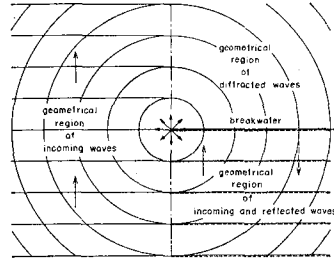


Fig.-3.1 Propagation pattern of geometrical waves

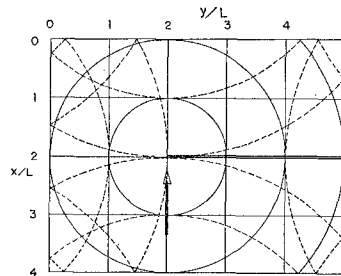


Fig.-3.2 Region of computation and propagation pattern of geometrical diffracted waves (after four periods)

lations. At the offshore imaginary boundary, the particle velocity of incident waves must be given at least two periods long to supply incident waves of four periods long to the breakwater.

This technique of calculation is equivalent to the practical method in hydraulic model experiments on waves as the measurements are finished before the time when re-reflected waves at the wave generator reach the model site of structures to keep the same condition of incident waves during the tests.

3.2 Difference equations

The non-dimensional basic differential equations are converted into following difference equations for the arrangement of computing points as shown in Fig.-3.3.

$$\left. \begin{aligned}
 \eta(i,j)^t + \Delta t/2 &= \eta(i,j)^t - \Delta t/2 \\
 &- \frac{\Delta t}{\Delta x} \{u(i+1,j)^t - u(i,j)^t\} \\
 &- \frac{\Delta t}{\Delta y} \{v(i,j+1)^t - v(i,j)^t\} \\
 u(i,j)^t + \Delta t &= u(i,j)^t \\
 &- \frac{\Delta t}{\Delta x} \{ \eta(i,j)^t + \Delta t/2 - \eta(i-1,j)^t + \Delta t/2 \} \\
 v(i,j)^t + \Delta t &= v(i,j)^t \\
 &- \frac{\Delta t}{\Delta y} \{ \eta(i,j)^t + \Delta t/2 - \eta(i,j-1)^t + \Delta t/2 \}
 \end{aligned} \right\} (3.1)$$

where the subscript $*$ which means the non-dimensional quantity is dropped to avoid unwieldy notation.

3.3 Initial and Boundary conditions

(1) Initial conditions

In this calculation, a sinusoidal wave train propagating in the negative direction of x axis is considered as the incident waves. The time when the front of the incident wave train reaches the front of breakwater ($i = i_0$) is counted zero, then the following initial conditions are given from the conventional small amplitude wave theory.

Initial calm region ($i < i_0$)

$$\left. \begin{aligned}
 \eta(i,j)^{-\Delta t/2} &= 0 \\
 u(i,j)^0 &= 0 \\
 v(i,j)^0 &= 0
 \end{aligned} \right\} (3.2)$$

Initial wave region ($i \geq i_0$)

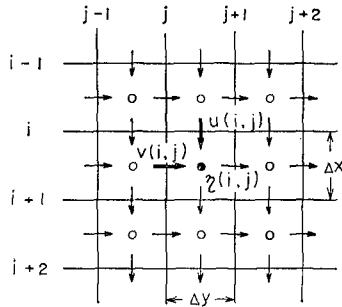


Fig.-3.3 Arrangement of computing points

$$\left. \begin{aligned} \eta(i,j)^{-\Delta t/2} &= \sin \left\{ 2\pi \left\{ (i-i_0)\Delta x + \frac{\Delta x}{2} - \frac{\Delta t}{2} \right\} \right\} \\ u(i,j)^0 &= -\sin \{ 2\pi(i-i_0)\Delta x \} \\ v(i,j)^0 &= 0 \end{aligned} \right\} \quad (3.3)$$

(2) Boundary conditions

There are two types of boundaries in the computing plane; the one is the imaginary boundary and the other is the internal boundary corresponding to the breakwater. At the offshore imaginary boundary, the velocity of incident waves is given and at the other three sides the velocity component is given zero.

Offshore boundary condition*

$$u(i_e, j)^{n\Delta t} = -\sin n\theta \quad (3.4)$$

where,

$$\left. \begin{aligned} \cos \theta &= 1 - \left(\frac{\Delta t}{\Delta x} \right)^2 (1 - \cos \phi) \\ \phi &= 2\pi\Delta x \end{aligned} \right\} \quad (3.5)$$

Internal boundary condition

$$V_n \Big|_s = 0 \quad (3.6)$$

where s is the circumference of the internal boundary and V_n is the normal velocity component to it.

Equation (3.6) is the condition for the boundary of perfect reflection. The condition of boundary with arbitrary reflecting power will be treated in 4.3.

3.4 Stability condition of numerical calculation

A following relation between the space interval x , y and the time interval t must be satisfied to perform stable calculations.

$$\Delta t \leq \frac{1}{\left(\frac{1}{\Delta x} + \frac{1}{\Delta y} \right)^{1/2}} \quad (3.7)$$

All the calculation in present paper are conducted by using following intervals,

$$\Delta x = \Delta y = \Delta s = \frac{1}{15}$$

$$\Delta t = \frac{1}{24}$$

* This is the velocity obtained as a solution of difference equations of which the initial conditions are given by Eq.(3.3) in the initial wave region. Details can be referred to the reference paper (5).

4. WAVE HEIGHT DISTRIBUTION ALONG A BREAKWATER

4.1 Comparison with analytical solutions

The diffraction pattern around a semi-infinite breakwater has been solved as the Sommerfeld solution and also around a detached breakwater has been obtained by solving the Mathieu equation. It has been already confirmed that these analytical solutions agree well with hydraulic model experimental results. The applicability of our numerical method to wave diffraction, therefore, can be verified by comparing the computed wave heights with those obtained from the conventional analytic solutions for a semi-infinite breakwater or a detached breakwater.

- For this purpose, the following three calculations are conducted,
- 1) a semi-infinite breakwater, normal incident wave direction ($\theta = 90^\circ$)
 - 2) a detached breakwater, normal incident wave direction ($\theta = 90^\circ$)
 - 3) a semi-infinite breakwater, oblique incident wave direction ($\theta = 45^\circ$)

(1) Wave height distribution along a semi-infinite breakwater ($\theta = 90^\circ$)

The distribution of wave height calculated by our numerical analysis method is compared with that obtained from the conventional analytic solution in Fig.-4.1. The wave heights in the numerical analysis are calculated at the computing points apart from the faces of the breakwater by $\Delta s/2$ ($= L/30$, in this case), because of the finite difference. Analytical solutions both at the face of the breakwater and at the computing points of water elevation are shown.

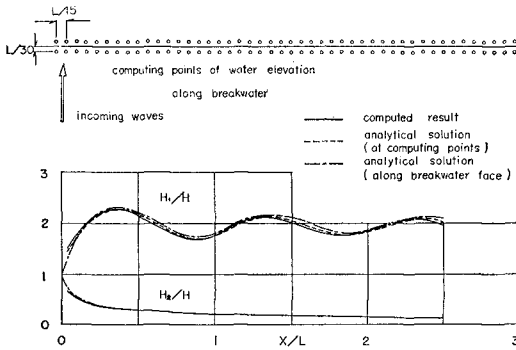


Fig.-4.1 Wave height distribution along a semi-infinite breakwater

The undular distribution of wave height along the front face is well realized in the calculated result as predicted by the analytical solution. The wave height distribution along the rear face of breakwater by both methods extremely agree with each other.

(2) Wave height distribution along a detached breakwater ($\theta = 90^\circ$)

The wave height distribution along a detached breakwater of which the

length is $2L$ is calculated for the incident waves approaching normally to it.

Fig.-4.2 shows the comparison of results obtained by the numerical analysis and by the conventional solution. A little difference around the tip of breakwater may be due to the difference of calculating points.

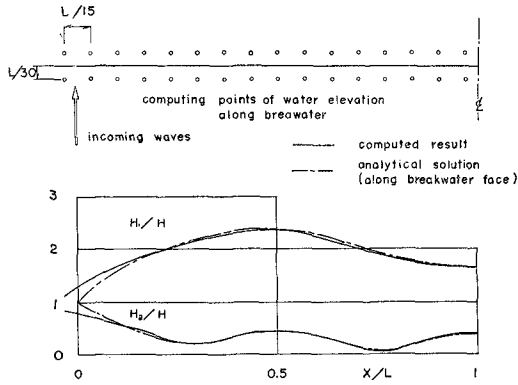


Fig.-4.2 Wave height distribution along a breakwater with the length of $2L$

(3) Wave height distribution along a semi-infinite breakwater ($\theta = 45^\circ$)

We take the direction of incident waves on one axis of the grid system and make the oblique breakwater bear a close resemblance to a staircase shape. The results are shown in Fig.-4.3 where the staircase breakwater

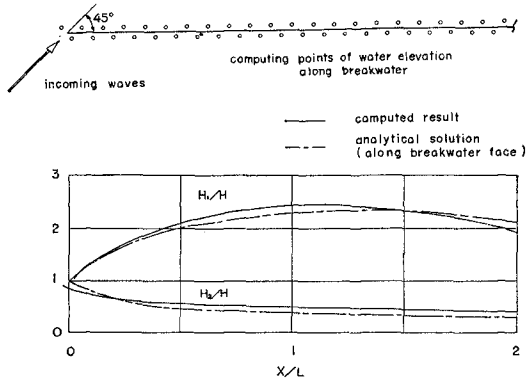


Fig.-4.3 Wave height distribution along a semi-infinite breakwater due to obliquely incoming waves

is drawn as a straight line. Some difference is noticed between the calculated result and the analytical solution. This degree of difference, however, could be reduced by using finer space intervals.

4.2 Wave height distribution along a breakwater of arbitrary shape

As an example of application to a breakwater of arbitrary shape, the distribution of wave height along a semi-infinite breakwater with a short wing is calculated.

Fig.-4.4 shows the calculated result for the case the length of the short wing is 0.4L and the direction of incident waves is normal to the main part of the breakwater. It is noticed apparently that the non-uniformity of wave height is increased due to the existence of the short wing.

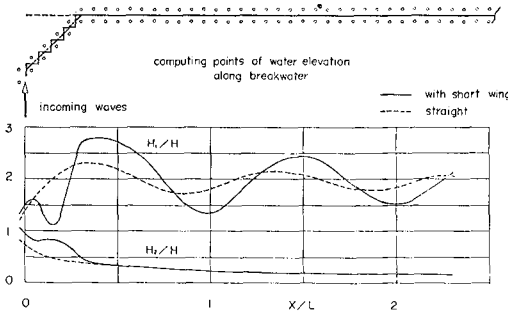


Fig.-4.4 Wave height distribution along a semi-infinite breakwater with a short wing

4.3 Wave height distribution along a breakwater of arbitrary reflecting power

There exists a number of breakwaters which are not of perfect reflection, for examples, rubble mound breakwaters and vertical walls protected by artificial blocks. For these breakwaters, the authors have devised a special calculation way named the Wave generator method.

Let us explain the principle of the wave generator method for a straight breakwater of perfect reflection. In this case, the velocity potential can be expressed as a sum of the velocity potential of incident waves (ϕ_i) and that of scattered waves by the breakwater (ϕ_d),

$$\phi = \phi_i + \phi_d \tag{4.1}$$

Furthermore, since the scattered waves can be considered as a sum of waves generated at the front face (ϕ_f) and at the rear face of the breakwater (ϕ_r), ϕ_d is expressed as,

$$\phi_d = \phi_f + \phi_r \tag{4.2}$$

We can interpret obviously that waves generated at the front face are waves corresponding to reflected waves by the breakwater and waves generated at the rear face are waves cancelling the incident waves. Such waves must be generated at the both faces of the breakwater so as to satisfy the following conditions;

$$\left. \frac{\partial \phi_f}{\partial n} \right|_s = - \left. \frac{\partial \phi_i}{\partial n} \right|_s \quad (4.3)$$

$$\left. \frac{\partial \phi_r}{\partial n} \right|_s = - \left. \frac{\partial \phi_i}{\partial n} \right|_s \quad (4.4)$$

where s designates the circumference of the breakwater and n designates the normal direction to it.

Since the breakwater is replaced by a special wave generator, the authors have named this calculation way the Wave generator method. In this method, the calculation is performed by following procedure;

- 1) Calculation of incident waves in the absence of breakwater
- 2) Calculation of waves generated by the hypothetical wave generator at the boundary of the breakwater, by using the calculated velocity component of incident waves in 1)
- 3) Summation of simultaneous results of incident waves and generated waves

The wave height distribution along a semi-infinite breakwater which was calculated by this wave generator method has been confirmed to agree perfectly with that obtained by the ordinary calculation method of our numerical analysis.

In case that the arbitrary reflection coefficient $r(s)$ distributes along the face of a breakwater, the following equation is used for Eq. (4.3),

$$\left. \frac{\partial \phi_f}{\partial n} \right|_s = - r(s) \left. \frac{\partial \phi_i}{\partial n} \right|_s \quad (4.5)$$

It should be noted that this wave generator method is directly applied only to the case in which velocities of all the incoming waves with normal component to the boundary can be obtained. As to the case of the semi-infinite breakwater, both waves generated at the front face and waves generated at the rear face are propagating along the breakwater when they reach the other face and they have no normal velocity component to it. Therefore, it is enough that only incident waves are considered as incoming waves to the breakwater.

However, if there are two separate breakwaters, and waves generated at one of the breakwaters reach the other with normal velocity component to it, it is necessary to repeat the calculation procedure at any computing time step.

Fig.-4.5 shows the wave height distribution along a semi-infinite breakwater of perfect reflection, of no reflection along the breakwater, and of no reflection only at the heading part. Two remarks are pointed out from these results: 1) The wave height in the vicinity of no reflection part is approximately equal to that of the incident wave at the front face. 2) Little effect of the reflecting power is brought on the wave height along the rear face.

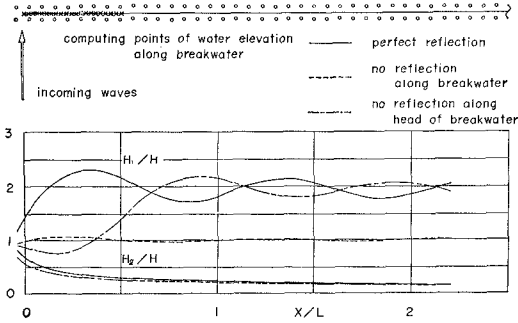


Fig.-4.5 Effect of reflecting power on wave height distribution

4.4 Application to wave force upon a large isolated vertical structure

An interesting application of our method of numerical analysis is the calculation of wave force upon a large isolated vertical structure of arbitrary shape.

Components of wave force upon a structure can be obtained from the following relation, when the water surface elevation along the structure is calculated by the numerical analysis,

$$F_x = \oint_{-h}^0 \rho dz \cdot l(s) ds = \frac{\rho g}{k} \tanh kh \oint_{-h}^0 l(s) ds$$

$$F_y = \oint_{-h}^0 \rho dz \cdot m(s) ds = \frac{\rho g}{k} \tanh kh \oint_{-h}^0 m(s) ds$$

(4.6)

where s is the circumference of the structure and (l,m) is the directional cosine of the inward normal line.

As an example of application, wave force upon a rectangular body which

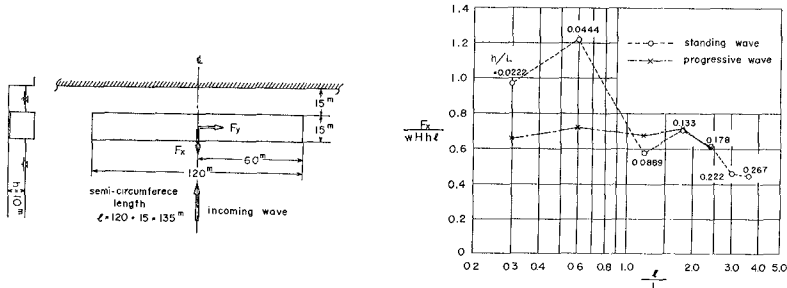


Fig.-4.6 Arrangement of a rectangular vertical body and calculated wave force

is a simplified treatment for a moored ship is calculated. Fig.-4.6 shows the arrangement of the moored ship and calculated wave forces with and without a vertical quay wall of infinite length.

5. APPLICATION TO THE REGION OF VARIABLE WATER DEPTH

5.1 Correction factor of shoaling

For the propagation of waves in the region of variable water depth $h(x,y)$, we assume that the wave frequency σ is constant and the local wave number k is given by Eq.(2.10). Then, our wave equations include the variation of wave height due to shoaling caused by the variation of water depth as well as due to refraction caused by the variation of wave phase velocity.

The variation of wave height due to shoaling, however, is not the function of the group velocity but of the phase velocity in our wave equations.

As a simple example of water depth variation, let us consider the region where the water depth changes in step-shape at $x = 0$ from h_1 to h_2 as shown in Fig.-5.1.

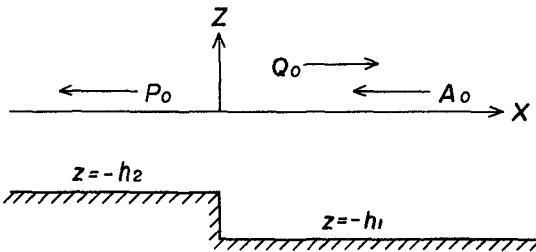


Fig.-5.1 Change of water depth in step-shape

The velocity potential for this situation is expressed in the following form,

$$\left. \begin{aligned} \phi_1 &= (A_0 e^{ikx} + Q_0 e^{-ikx}) e^{i\sigma t} \frac{\cosh k(z+h_1)}{\cosh kh_1} \\ &+ \sum_{m=1}^{\infty} A_m e^{-k_m x} e^{i\sigma t} \frac{\cosh k_m(z+h_1)}{\cosh k_m h_1}, \quad x \geq 0 \\ \phi_2 &= P_0 e^{ik'x} e^{i\sigma t} \frac{\cosh k'(z+h_2)}{\cosh k' h_2} \\ &+ \sum_{n=1}^{\infty} P_n e^{k'_n x} e^{i\sigma t} \frac{\cosh k'_n(z+h_2)}{\cosh k'_n h_2}, \quad x \leq 0 \end{aligned} \right\} (5.1)$$

And,

$$\begin{aligned} \sigma^2 &= k g \tanh kh \\ &= -k_m g \tanh k_m h \end{aligned} \tag{5.2}$$

Unknown coefficients in Eq.(5.1) can be determined from the following boundary conditions at $x = 0$,

$$\begin{aligned} \phi_1 &= \phi_2 \quad , (\text{continuity of pressure}) \\ \frac{\partial \phi_1}{\partial x} &= \frac{\partial \phi_2}{\partial x} \quad , (\text{continuity of horizontal particle velocity}) \end{aligned} \tag{5.3}$$

As obvious from Eq.(5.1), the strict solution includes an infinite series and the term of group velocity c_g appears through mathematical development for the determination of unknown coefficients. Waves corresponding to the infinite series, however, are not progressive waves and does not contribute the energy transport over one period. Consequently, the following relation of energy conservation can be obtained,

$$p^2 c_{g*} + q^2 = 1 \tag{5.4}$$

where,

$$\begin{aligned} p &= \left| \frac{P_0}{A_0} \right| \quad , (\text{transmission coefficient}) \\ q &= \left| \frac{Q_0}{A_0} \right| \quad , (\text{reflection coefficient}) \\ c_{g*} &= c_{g2} / c_{g1} \end{aligned}$$

The c_{g1} and c_{g2} are the group velocities respectively in the region of water depth h_1 and h_2 , and the group velocity is given by,

$$c_g = nc = \frac{1}{2} \left(1 + \frac{2kh}{\sinh 2kh} \right) c \tag{5.5}$$

The basic wave equations of our method of numerical analysis include only waves corresponding to the first term of the strict solution Eq.(5.1) and does not include waves corresponding to the infinite series.

Now we consider the analytic solution of our wave equations for the situation as shown in Fig.-5.1. Starting from the finite difference equations, the following coefficients of transmission and reflection are obtained,

$$\begin{aligned} p &= \frac{2}{1 + c_*} \\ q &= \left| \frac{1 - c_*}{1 + c_*} \right| = | p - 1 | \end{aligned} \tag{5.6}$$

where,

$$c_* = c_2 / c_1$$

From these relations, we get

$$p^2 c_* + q^2 = 1 \tag{5.7}$$

Comparing Eq.(5.7) with the strict solution of Eq.(5.4), it is noticed that the group velocity in Eq.(5.4) is replaced by the phase velocity in Eq.(5.7).

If reflection can be neglected, the transmission coefficient is written as,

$$p = c_{g*}^{-1/2} \quad , \text{ from Eq.(5.4)} \quad (5.8)$$

$$p = c_*^{-1/2} \quad , \text{ from Eq.(5.7)} \quad (5.9)$$

This relation is kept for a sloping bottom, if reflection is neglected, and the coefficient of Eq.(5.8) is equivalent to the conventional shoaling factor. To keep this conventional relation of shoaling factor, therefore, the shoaling factor in our analysis should be multiplied with the following correction factor of shoaling,

$$f_s = n_*^{-1/2} \left\{ \left(1 + \frac{2k_1 h_1}{\sinh 2k_1 h_1} \right) / \left(1 + \frac{2kh}{\sinh 2kh} \right) \right\}^{1/2} \quad (5.10)$$

When the deep water is taken as a reference region, this value of correction factor varies from 1 in deep water to 0.707 in the region of long waves.

In the application of our method of numerical analysis to a submerged shoal with concentric circular contours which is treated in the next section, final results of wave height are multiplied with this correction factor of shoaling.

5.2 Wave height distribution in the vicinity of ray intersections

Since the conventional wave refraction theory is based on the geometrical optic approximation, it fails to predict wave height at and near caustics where ray intersections occur. It has been already pointed out that the effect of diffraction in wave refraction should be included in the analysis of waves in the vicinity of ray convergence. Our method of numerical analysis is applicable to the region where caustics are formed.

As an example , our method is applied to wave propagation on a submerged shoal with concentric circular contours where the conventional refraction theory indicates the formation of a cusped caustics as shown in Fig.-5.2.

Figure 5.3 shows the arrangement of the shoal in the numerical calculation.

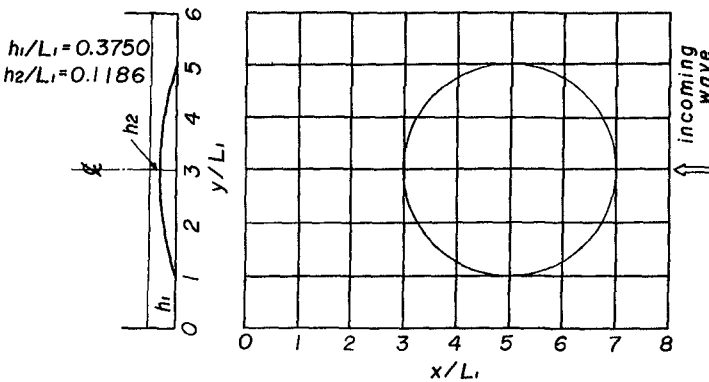


Fig.-5.3 Arrangement of a shoal

Hydraulic model experiments for same situation are conducted to confirm the validity of our method. The water depth and the wave length in the model are as follows,

$$h_1 = 15 \text{ cm}, h_2 = 5 \text{ cm}, L_1 = 40 \text{ cm}.$$

All tests are conducted for non-breaking waves.

Both results of the numerical calculation and the hydraulic model tests are presented in Fig.-5.4, 5.5, and 5.6. In Fig.-5.4, the wave height which is not corrected for the shoaling factor is also shown. It is noticed that experimental results agree better with the corrected value than that of non-correction. Maximum wave height in the calculated results is $2.1 H_1$ near the rear end of the shoal.

6. SUMMARY AND CONCLUSIONS

A method has been presented to obtain numerically wave patterns in any region of arbitrary shape from deep water to shallow water. The principle is to solve the linearized wave equations under the given boundary conditions from a certain initial state, which are derived from the Eulerian equations of motion and of continuity and include only unknown functions at the water surface.

By applying our method of numerical analysis, it is possible to investigate various problems of wave propagation in the region of arbitrary shape and of variable water depth. In this paper, we have presented several examples of application of our method to wave diffraction and to wave refraction in the fundamental fashion.

The applicability of our method to wave diffraction has been confirmed by the comparison of the distribution of wave height along a semi-infinite breakwater and a detached breakwater by our numerical method with that obtained from the conventional analytic solutions. As an example of application to a breakwater of arbitrary shape, the distribution of wave height along a semi-infinite breakwater with a short wing is calculated. The result shows that the non-uniformity of wave height along the breakwater is apparently increased due to the existence of the short wing.

For a breakwater of arbitrary reflecting power, a modified method which is named the "Wave generator method" is devised. Two examples of application of this modified method to semi-infinite breakwaters of no reflection and of no reflection only at the heading part are shown. The effect of reflecting power on the wave height distribution along the rear side of the breakwater is a little.

In addition, an interesting application of our method with respect to wave diffraction is the calculation of wave force upon a large isolated vertical structure of arbitrary shape. As an example of application, wave forces upon a rectangular body which is regarded as a moored ship are calculated with and without a vertical quay wall behind the body.

As to the application to the region of variable water depth, the correction factor of shoaling has been introduced, since the shoaling factor for our basic wave equations is a function of the phase velocity instead of the group velocity in the conventional relation. This value of correction factor varies from 1 in deep water to 0.707 in the region of long waves, when the deep water is taken as a reference region.

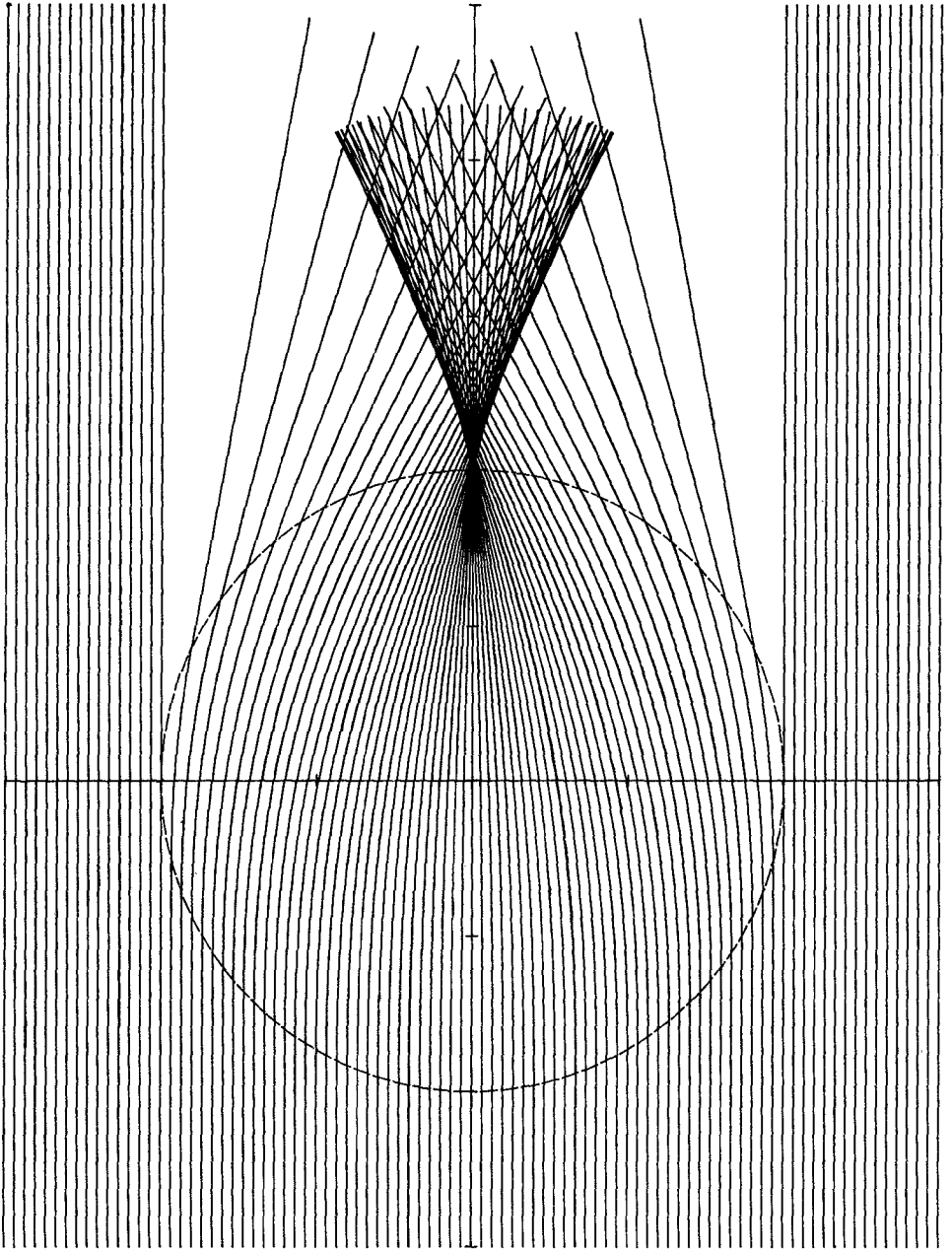


Fig.-5.2 Formation of a cusped caustics

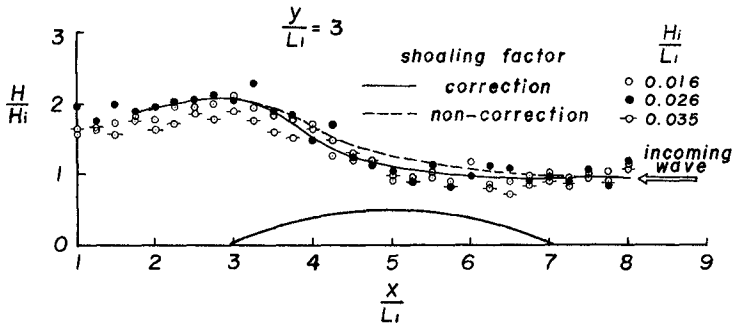


Fig.-5.4 Comparison of calculated wave height and experimental results (1)

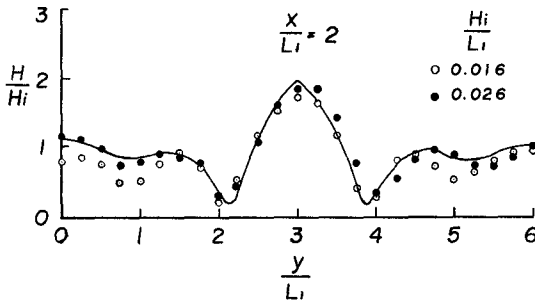


Fig.-5.5 Comparison of calculated wave height and experimental results (2)

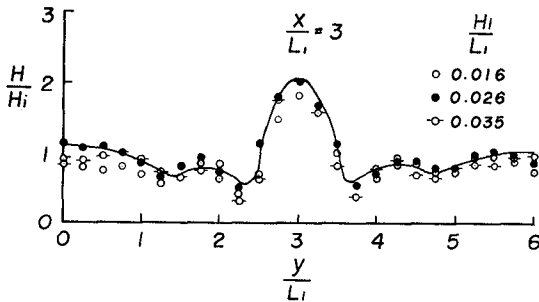


Fig.-5.6 Comparison of calculated wave height and experimental results (3)

Our method of numerical analysis is applicable to the analysis of wave propagation in the region of ray convergence. An example of application is shown to a submerged shoal with concentric circular contours where the conventional geo-optic wave refraction theory indicates the formation of a cusped caustics. Hydraulic model experiments are conducted to verify the validity of our method for a caustic problem. Calculated wave heights agree very well with those obtained from the model tests. The maximum wave height is $2.1 H_1$ at the rear end of the shoal where the geo-optic refraction theory gives the infinite wave height.

Our method of numerical analysis might be applied to the calculation of wave patterns in the region of more realistic bottom topography and it is possible to include vertical boundaries of arbitrary shape.

REFERENCES

- 1) Biesel, F., R. Ranson : Calculs de diffraction de la houle, Congrès de l'A.I.R.H., 1961
- 2) Gaillard, P. : Sur l'amplitude de la houle émise par une source ponctuelle isotrope dans un domaine de profondeur variable, La Houille Blanche, No.5, 1964
- 3) Barailler, L., P. Gaillard : Évolution récente des modèles mathématiques d'agitation due à la houle. Calcul de la diffraction en profondeur non uniforme, La Houille Blanche. No.8, 1968
- 4) Berkhoff, J.C.W. : Computation of combined refraction-diffraction, 13th International Conference on Coastal Engineering, 1972, Conference Abstracts
- 5) Fuku-uchi, H., Y. Ito : On the effect of breakwaters against tsunami, Proc. 10th Conference on Coastal Engineering, 1966
- 6) Ito, Y. : On the effect of Ofunato tsunami-breakwater against 1968 Tsunami, Proc. 13th Congress of IAHR, 1969
- 7) Ito, Y. : Head loss at tsunami-breakwater opening, Proc. 12th Conference on Coastal Engineering, 1970
- 8) Ito, Y. : On the effect of tsunami-breakwater, Coastal Engineering in Japan, Vol.13, 1970
- 9) Pierson, W.J.Jr. : The interpretation of crossed orthogonals in wave refraction phenomena, Technical Memorandum No.21, Beach Erosion Board, Corps of Engineers, 1951
- 10) Chao, Y.Y. : The theory of wave refraction, including the effects of caustics and spherical earth, Tech. Rept., TR-70-7, New York University, Geophysical Research Labs., 1970
- 11) Chao, Y.Y., W.J. Pierson, Jr. : An experimental study of gravity wave behavior near a straight caustic, Tech. Rept., TR-70-17, New York University, Geophysical Research Labs., 1970
- 12) Whalin, R.W. : Wave refraction theory in a convergence zone, 13th International Conference on Coastal Engineering, 1972, Conference Abstracts
- 13) Biesel, F. : Réfraction de la houle avec diffraction modérée, 13th International Conference on Coastal Engineering, 1972, Conference Abstracts